Optimizing Polar Codes Compatible with Off-the-Shelf LDPC Decoders

Moustafa Ebada, Ahmed Elkelesh and Stephan ten Brink
Institute of Telecommunications, Pfaffenwaldring 47, University of Stuttgart, 70569 Stuttgart, Germany
{ebada,elkelesh,tenbrink}@inue.uni-stuttgart.de

arXiv:1909.12030v1 [cs.IT] 26 Sep 2019

***Abstract*—Previous work showed that polar codes can be decoded using off-the-shelf LDPC decoders by imposing special constraints on the LDPC code structure, which, however, resulted in some performance degradation. In this paper we show that this loss can be mitigated; in particular, we demonstrate how the gap between LDPC-style decoding and Arıkan's Belief Propagation (BP) decoding of polar codes can be closed by taking into account the underlying graph structure of the LDPC decoder while jointly designing the polar code and the parity-check matrix of the corresponding LDPC-like code. The resulting polar codes under conventional LDPC-style decoding are shown to have similar error-rate performance when compared to some well-known and standardized LDPC codes. Moreover, we obtain performance gains in the high SNR region.**

I. Introduction

Polar codes, proposed in [1], are known to be the first class of error-correcting codes that is theoretically proven to be asymptotically capacity-achieving under successive cancellation (SC) decoding. In the ongoing 5^{th} generation mobile communication (5G) standardization process, the 3rd generation partnership project (3GPP) group has decided to deploy polar codes for the uplink and downlink control channel of the enhanced Mobile Broadband (eMBB) service [2], while discussion about deploying polar codes for massive machine-type communications (mMTC) and ultra-reliable low-latency communications (URLLC) is still ongoing. Therefore, developing practical decoders that satisfy the requirements defined by 5G new radio (5G-NR) has been progressively very intense, active and demanding. One of the issues targeted by 5G-NR is that it should have latency of less than 1 ms compared to 10 ms of 4G systems [3]. This latency reduction is required to enable the newly targeted applications of 5G systems such as augmented reality and 3D video rendering.

The fact that the SC decoder of polar codes suffers from a weak error-rate performance for finite-length codes has urged the development of further decoders. In [4], the SC decoder was extended to a successive cancellation list (SCL) decoder by applying the list decoding scheme on the plain SC decoder leading to an improved error-rate performance, close to the maximum likelihood (ML) bound for sufficiently large list sizes, on the cost of increased complexity. It was observed that in order not to miss the correct codeword in the list, a high-rate cyclic redundancy check (CRC) could be concatenated with the polar code and used while decoding, or just at the very end, as a path tag (i.e., distributed or non-distributed CRC, respectively), explaining the name CRC-aided successive cancellation list (CA-SCL). This concatenation leads to significant performance gains over state-of-the-art low-density parity-check (LDPC) and turbo codes. The concatenation of a polar code with a high-rate parity-check code was likewise introduced in [5] and [6] and shown to be of similar error-rate performance as of the CRC-aided polar codes, with more simplicity and flexibility. The resultant codes enjoy better weight spectrum properties [7] which is regarded as one reason for the improved performance. The performance of polar codes (i.e., both *plain* and *CRC-aided*) were further pushed forward by tailoring the designed polar code to both specifics of the code and decoder [8] at the cost of reduced code flexibility and increased code design complexity (i.e., offline complexity).

A major drawback of SC-based decoders is the high decoding latency and, thus, their low throughput due to the sequential decoding manner. To combat that, various SC-based decoding schemes were proposed, e.g., [9] and [10], mostly based on identifying specific node patterns and efficiently utilizing them to speed up the decoding process. Besides, for an SCL decoder, there is an increased implementation complexity (e.g., hardware complexity, memory requirements, etc.) proportional to the list size deployed. For that, more simplified variations were introduced, e.g., [7] and [11], limiting the increase in complexity, with only minimal performance loss in some cases. Furthermore, these classes of decoders do not provide soft-in/soft-out information processing which limits their usage in iterative detection and decoding schemes.

Usually a standard does not define a certain decoding technique and, thus, improved decoding algorithms (in terms of performance, complexity or throughput) may result in a competitive advantage. There exists another family of polar decoders, namely iterative decoders, which do not have the aforementioned problems. This class of decoders could be potentially suitable for high data rate applications (i.e., in particular from an implementation point of view). The first iterative decoder proposed was the belief propagation (BP) decoder [12] which was conducted on the factor graph that corresponds to the polarization matrix of the code. However, this decoder has an error-rate performance which is inferior to that of the CA-SCL decoder. One further step was made in [13], where a belief propagation list (BPL) decoder was introduced, with an improved error-rate performance compared to any other known-thus-far iterative decoder, however, while still being inferior to CA-SCL in terms of error-rate performance; this can be attributed to the CRC incompatibility and the non-

This work has been supported by DFG, Germany, under grant BR 3205/5-1.

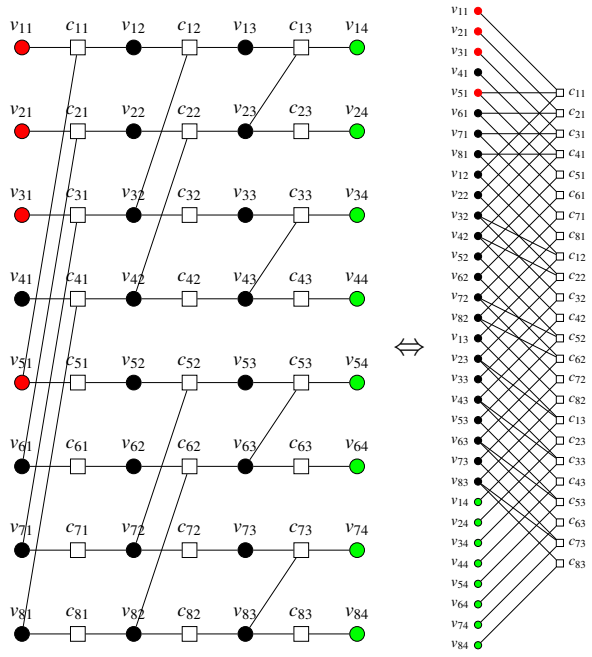


Fig. 1: Different BP decoder factor graph representations for a $\mathscr{P}(8,4)$-code with information set $\mathbb{A} = \{4,6,7,8\}$.

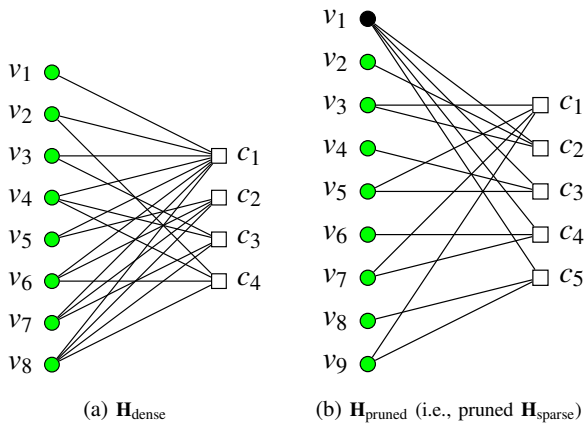
optimal code design in the case of the BPL decoder.

In this work, we use the Genetic Algorithm (GenAlg) to find (design) better polar codes (i.e., information/frozen sets) tailored to LDPC-style BP decoding. Also, we investigate the effect of changing the information/frozen set on the graphical representation of the underlying polar code which is used to run the BP algorithm.

II. Polar Codes Interpreted as LDPC Codes

Polar codes can be interpreted as LDPC codes with an underlying sparse Tanner graph [14]. This is illustrated in Fig. 1, Arıkan's original factor graph on the left and its corresponding bipartite factor graph, i.e., $\mathbf{H}_{\text{sparse}}$, on the right. With some basic pruning techniques, the size of the bipartite graph can be significantly reduced and made practical to use. This means that *any* polar code (e.g., the polar code considered in the 5G standard) can be surprisingly decoded using *conventional, off-the-shelf* LDPC decoders, e.g., based on the sum-product algorithm (SPA), given that we impose some constraints on the underlying LDPC code structure. On the one hand, this has the great advantage of re-using the existing hardware implementations of LDPC decoders, in addition to making use of the available systematic LDPC analysis and design tools; and enjoying all complexity, memory requirements and latency being significantly reduced. On the other hand, this way of interpreting/decoding the polar code has the drawback of degraded error-rate performance when compared to the conventional BP decoder [14, Fig. 1]. The decoding complexity of the LDPC-style decoder was significantly improved in [15] by means of deep learning with further enhanced throughput.

In this work, we show that one reason of the performance degradation when compared to the conventional BP decoder is attributed to the fact that the design of both – polar code and its corresponding LDPC parity-check matrix – do not take



(a) $\mathbf{H}_{\text{dense}}$ (b) $\mathbf{H}_{\text{pruned}}$ (i.e., pruned $\mathbf{H}_{\text{sparse}}$)

Fig. 2: Dense vs. sparse/pruned Tanner graphs for a $\mathscr{P}(8,4)$-code with information set $\mathbb{A} = \{4,6,7,8\}$.

into consideration the new decoding schedule (e.g., iterative manner, graph structure, scheduling, maximum number of iterations $N_{it,max}$ etc.). In addition to that, in this paper, we optimize the pruned parity-check matrix of the corresponding LDPC code to outperform the conventional BP decoder of polar codes over a wide signal-to-noise-ratio (SNR) range and approach the performance of the SCL decoder at higher SNR range. We compare the newly obtained codes to the original ones to provide some reasoning why the designed codes are better. We discuss this in terms of the weight spectrum of the newly obtained codes in addition to the girth profile and the degree distribution of the underlying parity-check matrices, which are also shown to benefit from a reduced size and, thus, reduced complexity. Finally, the special types of "hidden" nodes introduced in [14] are interpreted as punctured variable nodes and put into context within the design process.

Given the polarization matrix $\mathbf{G}_N$ of a polar code recursively constructed based on the $\mathbf{G}_2$ polarizing kernel, the parity-check matrix denoted as $\mathbf{H}_{\text{dense}}$ is formed from the columns of $\mathbf{G}_N$ with indices in $\bar{\mathbb{A}}$, where $\bar{\mathbb{A}}$ is the set of frozen indices, as proven in [16, Lemma 1]. Note that, the corresponding factor graph of $\mathbf{H}_{\text{dense}}$ is not sparse and, thus, it is not possible to apply the traditional decoding algorithms (e.g., SPA decoding) on the naive $\mathbf{H}_{\text{dense}}$, see Fig. 2a.

As depicted in [14, Fig. 4a], the $\log_2(N)+1$ sets of variable nodes (VNs) and $\log_2(N)$ sets of check nodes (CNs) in Arıkan's BP factor graph can be re-grouped into a bipartite graph consisting of *only* two sets: VNs $\mathscr{V}$ and CNs $\mathscr{C}$ [16]. Assuming the schedule is now the same as the conventional flooding BP of LDPC codes, the graph resembles an LDPC code with some special constraint. In [14], it was given the name "LDPC-like" to address the fact that the channel information bits of this LDPC code are only at the last N VNs. Applying some basic pruning, the graph can be significantly reduced with an approximate reduction factor of 80%. However, the final compact factor graph still contains a non-negligible portion of such nodes, called "hidden VNs", corresponding to the black VNs in Fig. 2b. In this work, these nodes are interpreted as punctured parity VNs of the LDPC code. Thus, taking into consideration the connections of these

punctured nodes to the rest of the graph while designing the code has an impact on the performance of the whole code as shown later. For more details on the pruning of the originally large bipartite graph, we refer the interested reader to [14, Sec. III] and the detailed source code provided online [17].

III. Code Construction Mismatch Paradigm

Polar code construction is the process of choosing the best k synthesized bit-channels out of the N synthesized bit-channels. The best k synthesized bit-channels are included in the information set $\mathbb{A}$ and are used for data transmission. Most of the state-of-the-art polar code construction algorithms are tailored to the hard-output SC decoder. For the case of an additive white Gaussian noise (AWGN) channel, they are based either on bounds (e.g., the Bhattacharyya parameter [1], density evolution [18]), approximations (e.g., Gaussian approximation (GA) [19]), or heuristics (e.g., polarization weight (PW) [20] and β-expansion [21]). It is worth-mentioning that an efficient density evolution-based implementation was proposed in [22]. There also exist several Monte-Carlo-based designs for specific decoding schemes. Additionally, various schemes focus on improving the finite-length performance of polar codes either by *interpolating* them using other codes (e.g., Reed–Muller (RM)-codes), to enjoy good finite-performance provided by these codes [23], [24] or via concatenation schemes with other codes, e.g., [25]–[27].

Furthermore, both iterative-specific parameters of the family of iterative decoders (e.g., scheduling, stopping sets, cycles, girths, etc.) and the list decoding fashion of SCL decoder variants are not usually considered in the polar code construction phase [28]. Therefore, this leaves the door wide open for optimizing the information set $\mathbb{A}$ and tailoring it to the decoder, thus, utilizing the decoder at the most efficient manner. This remark is even more significant in the finite-length regime where polar codes suffer from a degraded performance due to semi-polarized bit channels.

In [8], a new code construction framework for polar codes was presented where the Genetic Algorithm (GenAlg) was applied to the code construction optimization problem on a specific error-rate simulation environment, i.e., taking into consideration the actual decoder and channel. This *decoder-in-the-loop* design was shown to yield significant gains in terms of error-rate performance, where SCL performance was enhanced to achieve that of the CA-SCL even *without* using a CRC code, as shown in [8, Fig. 6].

Inspired by that, the GenAlg is applied to tailor the LDPC-like code, derived from the polar code, to the LDPC-style decoder and take into account its special constraints (i.e., the big set of punctured variable nodes). Due to limited space, we refer the interested reader to [8] and the pseudo-algorithms therein for specific details about the GenAlg framework.

IV. Results and Discussion

In this section, numerical results are presented in terms of both BER and BLER, as cost functions, to demonstrate the flexibility of our proposed algorithm. The optimized codes are compared at different lengths with standardized codes of the same corresponding block length and code rate. All considered polar and LDPC codes are simulated over the binary-input AWGN channel. In the following, by 5G polar codes we mean the bit-reliability order of the nested polar code with maximum code length $N_{max} = 1024$, specified by the 3GPP group in [29].

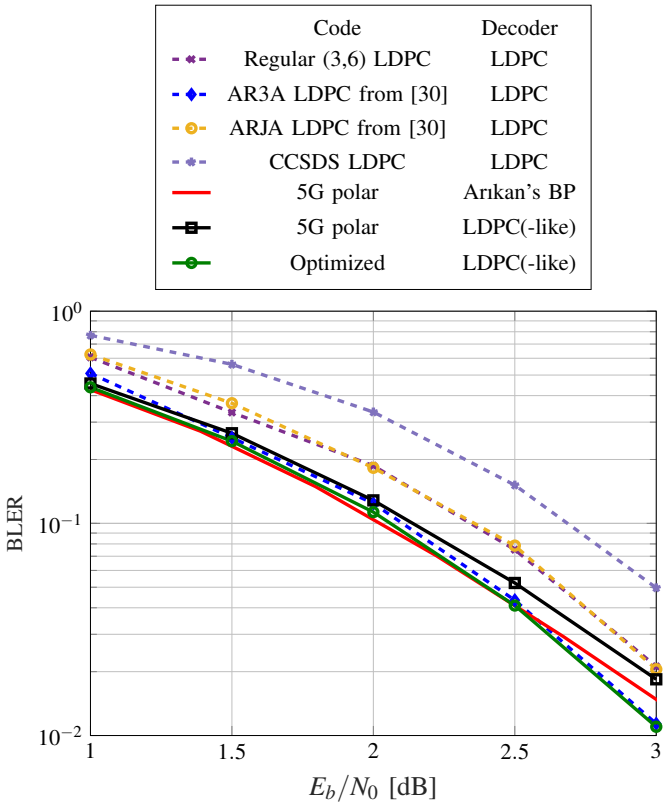


Fig. 3: BLER performance of the *optimized* $\mathscr{P}(128,64)$-code over the AWGN channel at $\mathrm{SNR}_{\mathrm{des}} = 3\,\mathrm{dB}$ under LDPC(-like) decoding. All iterative decoders use $N_{it,max} = 200$.

A. Codeword length $N = 128$

We design a $\mathscr{P}(128,64)$ polar code and its corresponding pruned sparse $\mathbf{H}_{\mathrm{pruned}}$ under LDPC-like decoding. All reference LDPC codes from [30] are designed through a girth optimization technique based on the PEG algorithm [31]: the standardized LDPC code by the Consultative Committee for Space Data Systems (CCSDS) for satellite telecommand links, an accumulate-repeat-3-accumulate (AR3A) LDPC code and an accumulate-repeat-jagged-accumulate (ARJA) LDPC code. A further reference code is the 5G polar code without the CRC-aid. As depicted in Fig. 3, the BLER performance of the BLER-optimized polar code under LDPC(-like) decoding achieves the performance of the 5G polar code under Arıkan's conventional BP decoder, with a performance gain of 0.25 dB at BLER of 10^{-2} compared to the originally proposed code in [14]. It outperforms the 5G polar code under Arıkan's conventional BP decoder in the higher SNR range.

Besides, it outperforms the LDPC codes presented in Fig. 3. It is, however, important to keep in mind that these codes have special constraints on their structure for implementation reasons (i.e., encoding complexity issues), yet, the message here is to show that the newly proposed codes are of comparable performance which brings them to attention for further

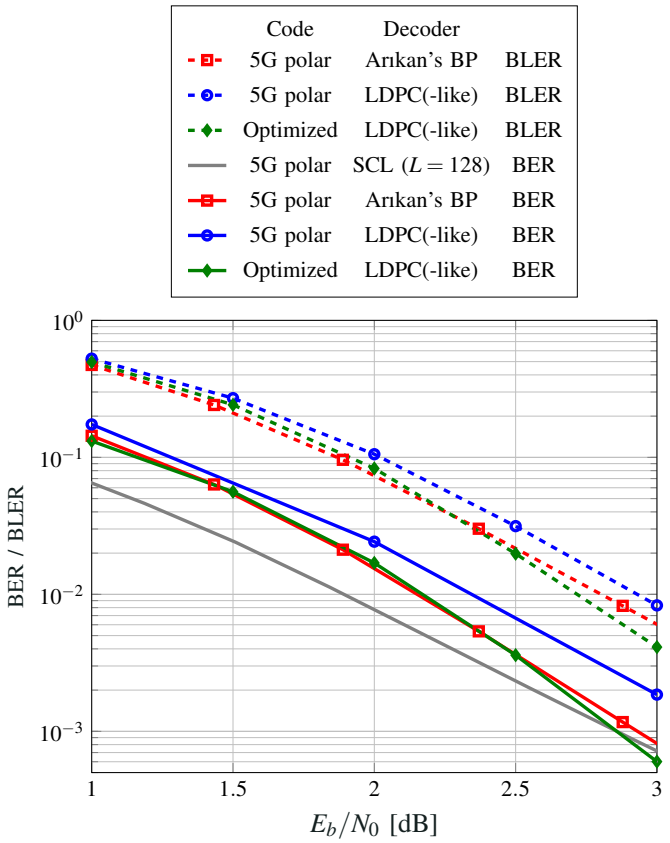


Fig. 4: BER/BLER performance of the *optimized* $\mathscr{P}(256,128)$-codes over the AWGN channel at $\text{SNR}_{\text{des}} = 3\,\text{dB}$ under LDPC(-like) decoding. All iterative decoders use $N_{it,max} = 200$ and no CRC is used.

improvements. Note that, the proposed code is encoded via a low-complexity polar encoder, despite being decoded by a conventional LDPC decoder.

Tab. I depicts a comparison between the minimum distance of both codes. It turns out that the optimized code has the same minimum distance as the initial 5G code, however, at a significantly reduced number of minimum-weight codewords $A_{d_{min}}$. This was computed using the algorithm proposed in [7] with a list size of up to $L = 5 \cdot 10^5$.

One more comparison providing insights on why the obtained code performs better is the girth of the optimized $\mathbf{H}$-matrix. Both $\mathbf{H}$-matrices of the initial 5G and the optimized code are of minimum girth-6. However, the optimized code has a reduced number of 1825 cycles of girth-6, when compared to the original $\mathbf{H}$-matrix corresponding to the 5G polar code of 2234 girth-6 cycles. Furthermore, the optimized $\mathbf{H}_{\text{opt}}$-matrix has a reduced size of 365×493 compared to an original size of $\mathbf{H}_{\text{pruned,5G}}$ of 503×633. Therefore, the number of punctured variable nodes has been minimized.

Tab. I: The number of minimum-weight codewords of a $\mathscr{P}(128,64)$-code

Construction	d_{min}	A_8
5G [29]	8	304
Optimized @ 3 dB	8	170

B. Codeword length $N = 256$

We design a $\mathscr{P}(256,128)$ polar code and its corresponding pruned sparse $\mathbf{H}_{\text{pruned}}$ under LDPC-like decoding with both BLER and BER as cost functions. The newly obtained codes are compared to the 5G polar code without the CRC-aid [29] under BP, LDPC-like and plain SCL decoding. As depicted in Fig. 4, both BER and BLER performance of the optimized codes under LDPC(-like) decoding achieve the performance of the 5G polar code under Arıkan's conventional BP decoder, with a performance gain of around 0.2 dB and 0.1 dB at BLER of 10^{-2} and BER of 10^{-3}, respectively, compared to the originally proposed code in [14]. They even outperform the 5G polar code under both Arıkan's conventional BP *and* plain SCL decoders towards a higher SNR range.

Tab. II depicts a comparison between the minimum distance of both codes (initial and BLER-optimized). It turns out that the BLER-optimized code has the same minimum distance as the initial 5G polar code, with significantly reduced number of minimum-weight codewords. These numbers were obtained using the algorithm in [7] with a list size up to $L = 2.5 \cdot 10^5$.

Tab. II: The number of minimum-weight codewords of a $\mathscr{P}(256,128)$-code

Construction	d_{min}	A_8
5G [29]	8	96
Optimized @ 3 dB	8	68

C. Codeword length $N = 512$

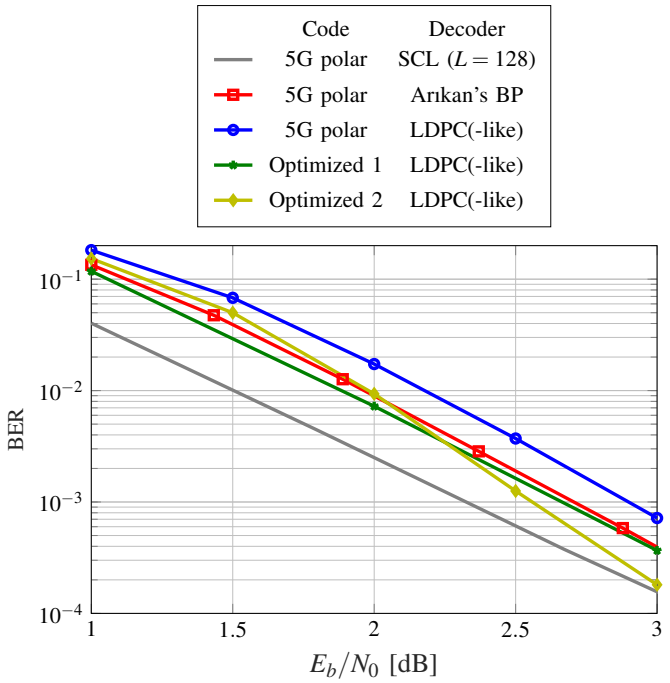
A $\mathscr{P}(512,256)$ polar code along with its corresponding sparse $\mathbf{H}_{\text{pruned}}$ are designed under LDPC-like decoding with BER as the cost function. The newly obtained code is compared to the 5G polar code without the CRC-aid [29], under BP, LDPC-like and plain SCL decoding. As depicted in Fig. 5a, BER performance of the optimized code under LDPC(-like) decoding achieve the performance of the 5G polar code under Arıkan's conventional BP decoder, with a performance gain of around 0.4 dB at BER of 10^{-3}, compared to the originally proposed code in [14]. It even outperforms the 5G polar code under Arıkan's conventional BP decoder, while approaching it under plain SCL in the high SNR range.

For this scenario, two optimization processes were conducted, at design SNRs 2.5 dB and 3 dB, resulting in code 1 and code 2, respectively. Depending on the desired SNR region (or error-rate level), one of them may be more suited to be applied. Furthermore, the convergence behavior (or epochs) of both processes is depicted in Fig. 5b and 5c, respectively.

It is worth-mentioning that the CRC-aided 5G polar codes under SCL decoding are of better error-rate performance than the state-of-the-art BP-based polar decoders. One reason is the CRC incompatibility in the iterative decoding environment.

V. Conclusion

An enhanced polar code design tailored to off-the-shelf LDPC decoders is presented. We attempt to design a suitable parity-check matrix such that polar codes could be decoded using an equivalent LDPC-like code. Thus, our proposed codes can be efficiently encoded with a low complexity polar encoder and can be decoded with a low complexity conventional (flooding schedule-based) BP LDPC decoder, also providing soft-outputs. Extensions to other LDPC decoders (e.g., min-sum approximation-based or quantized LDPC decoders) are



(a) BER comparison. All iterative decoders use $N_{it,max} = 200$.



(b) BER evolution of code 1 at $\mathrm{SNR}_{\mathrm{des}} = 2\,\mathrm{dB}$.



(c) BER evolution of code 2 at $\mathrm{SNR}_{\mathrm{des}} = 2.5\,\mathrm{dB}$.

Fig. 5: Optimized $\mathscr{P}(512,256)$-codes over the AWGN channel at $\mathrm{SNR}_{\mathrm{des}} = 2\,\mathrm{dB}$ and $2.5\,\mathrm{dB}$ under LDPC(-like) decoding and no CRC is used.

straightforward. Using our proposed design method, error-rate performance gains were achieved compared to the 5G polar codes under iterative decoding. We further showed that the gains can be attributed to the reduction in the number of minimum-weight codewords and other enhancements such as girth profile of the respective decoding graph and the reduced number of punctured variable nodes in it.

References

[1] E. Arıkan, "Channel Polarization: A Method for Constructing Capacity-Achieving Codes for Symmetric Binary-Input Memoryless Channels," *IEEE Trans. Inf. Theory*, vol. 55, no. 7, pp. 3051–3073, July 2009.

[2] Huawei, "Evaluation of TBCC and Polar Codes for Small Block Lengths," *3GPP TSG RAN WG1 N.85, Tech. Rep.*, May 2016.

[3] ——, "5G: New Air Interface and Radio Access Virtualization, Huawei white paper,," 2015. [Online]. Available: https://bit.ly/2IgpHv1(Accessdate:20.09.2018).

[4] I. Tal and A. Vardy, "List Decoding of Polar Codes," *IEEE Trans. Inf. Theory*, vol. 61, no. 5, pp. 2213–2226, May 2015.

[5] P. Trifonov and V. Miloslavskaya, "Polar Codes with Dynamic Frozen Symbols and Their Decoding by Directed Search," in *IEEE Inf. Theory Workshop (ITW)*, Sep. 2013, pp. 1–5.

[6] T. Wang, D. Qu, and T. Jiang, "Parity-Check-Concatenated Polar Codes," *IEEE Commun. Lett.*, vol. 20, no. 12, pp. 2342–2345, Dec. 2016.

[7] B. Li, H. Shen, and D. Tse, "An Adaptive Successive Cancellation List Decoder for Polar Codes with Cyclic Redundancy Check," *IEEE Commun. Lett.*, vol. 16, no. 12, pp. 2044–2047, Dec. 2012.

[8] A. Elkelesh, M. Ebada, S. Cammerer, and S. ten Brink, "Decoder-tailored Polar Code Design Using the Genetic Algorithm," *IEEE Trans. Commun.*, 2019.

[9] G. Sarkis, P. Giard, A. Vardy, C. Thibeault, and W. J. Gross, "Fast List Decoders for Polar Codes," *IEEE J. Sel. Areas Commun.*, vol. 34, no. 2, pp. 318–328, Feb. 2016.

[10] P. Giard and A. Burg, "Fast-SSC-Flip Decoding of Polar Codes," in *IEEE Wireless Commun. and Networking Conf. Workshops (WCNCW)*, Apr. 2018, pp. 73–77.

[11] S. A. Hashemi, M. Mondelli, S. H. Hassani, C. Condo, R. L. Urbanke, and W. J. Gross, "Decoder Partitioning: Towards Practical List Decoding of Polar Codes," *IEEE Trans. Commun.*, vol. 66, no. 9, pp. 3749–3759, Sep. 2018.

[12] E. Arıkan, "A Performance Comparison of Polar Codes and Reed-Muller Codes," *IEEE Commun. Lett.*, vol. 12, no. 6, pp. 447–449, June 2008.

[13] A. Elkelesh, M. Ebada, S. Cammerer, and S. ten Brink, "Belief Propagation List Decoding of Polar Codes," *IEEE Commun. Lett.*, vol. 22, no. 8, pp. 1536–1539, Aug. 2018.

[14] S. Cammerer, M. Ebada, A. Elkelesh, and S. ten Brink, "Sparse Graphs for Belief Propagation Decoding of Polar Codes," in *IEEE Inter. Symp. Inf. Theory (ISIT)*, June 2018, pp. 1465–1469.

[15] W. Xu, X. You, C. Zhang, and Y. Be'ery, "Polar Decoding on Sparse Graphs with Deep Learning," in *52nd Asilomar Conference on Signals, Systems, and Computers*, Oct. 2018, pp. 599–603.

[16] N. Goela, S. B. Korada, and M. Gastpar, "On LP Decoding of Polar Codes," in *IEEE Inf. Theory Workshop (ITW)*, Aug. 2010, pp. 1–5.

[17] "https://github.com/SebastianCa/LDPC-like-Decoding-of-Polar-Codes."

[18] R. Mori and T. Tanaka, "Performance of Polar Codes with the Construction using Density Evolution," *IEEE Commun. Lett.*, vol. 13, no. 7, pp. 519–521, July 2009.

[19] P. Trifonov, "Efficient Design and Decoding of Polar Codes," *IEEE Trans. Commun.*, vol. 60, no. 11, pp. 3221–3227, Nov. 2012.

[20] "3GPP, R1-167209, Polar code design and rate matching, Huawei, HiSilicon."

[21] G. He, J. C. Belfiore, I. Land, G. Yang, X. Liu, Y. Chen, R. Li, J. Wang, Y. Ge, R. Zhang, and W. Tong, "β-expansion: A Theoretical Framework for Fast and Recursive Construction of Polar Codes," in *IEEE Global Commun. Conf. (GLOBECOM)*, Dec. 2017, pp. 1–6.

[22] I. Tal and A. Vardy, "How to Construct Polar Codes," *IEEE Trans. Inf. Theory*, vol. 59, no. 10, pp. 6562–6582, Oct. 2013.

[23] B. Li, H. Shen, and D. Tse, "A RM-Polar Codes," *ArXiv e-prints*, July 2014.

[24] M. Mondelli, S. H. Hassani, and R. L. Urbanke, "From Polar to Reed-Muller Codes: A Technique to Improve the Finite-Length Performance," *IEEE Trans. Commun.*, vol. 62, no. 9, pp. 3084–3091, Sep. 2014.

[25] P. Trifonov and V. Miloslavskaya, "Polar Subcodes," *IEEE J. Sel. Areas Commun.*, vol. 34, no. 2, pp. 254–266, Feb. 2016.

[26] J. Guo, M. Qin, A. G. i Fàbregas, and P. H. Siegel, "Enhanced Belief Propagation Decoding of Polar Codes through Concatenation," in *IEEE Inter. Symp. Inf. Theory (ISIT)*, June 2014, pp. 2987–2991.

[27] A. Elkelesh, M. Ebada, S. Cammerer, and S. ten Brink, "Flexible Length Polar Codes through Graph Based Augmentation," in *IEEE Inter. ITG Conf. on Syst., Commun. and Coding (SCC)*, Feb. 2017.

[28] V. Bioglio, C. Condo, and I. Land, "Design of Polar Codes in 5G New Radio," *ArXiv e-prints*, Apr. 2018.

[29] "Technical Specification Group Radio Access Network," *3GPP, 2018, TS 38.212 V.15.1.1.* [Online]. Available: http://www.3gpp.org/ftp/Specs/archive/38_series/38.212/

[30] G. Liva, L. Gaudio, T. Ninacs, and T. Jerkovits, "Code Design for Short Blocks: A Survey," *ArXiv e-prints*, Oct. 2016.

[31] X.-Y. Hu, E. Eleftheriou, and D. M. Arnold, "Regular and Irregular Progressive Edge-Growth Tanner Graphs," *IEEE Trans. Inf. Theory*, vol. 51, no. 1, pp. 386–398, Jan. 2005.